# Open Stope design: State-of-the-art

**Suorineni, F.T.**
MIRARCO-Mining Innovation/Geomechanics Research Centre,
Laurentian University, 935 Ramsey Lake Road, Sudbury P3E 2C6, Ontario, Canada;
Tel: (705) 674-1151 ext. 5096; Fax: (705) 675-4838; email: fsuorineni@mirarco.org

**Abstract**

The stability graph method is the primary method for open stope design. The stability graph was introduced about three decades ago for bulk mining of orebodies below 1000-m depth. Since then, it has gained wide recognition around the world in hard rock metalliferous mining. Several developments aimed at improving its reliability in predicting the stability state of stopes have taken place. These developments include re-definition of the stability graph number factors, the transition zones, and addition of new factors. Various types of stability graphs have also emerged over the years for other purposes such as cablebolt layout design. The original database has also been significantly expanded from the original 26 cases in 1981 to 483 cases to date. This paper, critically reviews the developments of the stability graph to date with the objectives of:

- Synthesizing the scattered knowledge of these developments in the literature to a single source.
- Making potential users of the method aware of the problems and risks arising from the uncoordinated application of the method.
- Identifying areas for further research to improve the reliability of the method; and finally
- Providing guidelines to inexperienced users of the stability graph, and practitioners unaware of the various developments on when to use any one of the several stability graph types currently available.

The paper stresses that as an empirical method, the reliability of the stability graph is largely dependent on the size, quality and consistency of the database. The present tendency for authors to arbitrarily choose between the original and modified stability number factors, result in incomparable data that cannot be combined, while the different transition zones result in different interpretations of the stability state of a given stope surface thereby creating confusion. The review also shows that there is need for factors that account for stope stand-up

time, blast damage, and a gravity factor that is stress factor dependent. There is also a need to develop procedures for determining stability of open stope surfaces that are made of backfill. The inexperienced user and practitioner unaware of the various versions of the stability graph should be conscious of the different versions and types of stability graphs in order to make the appropriate choice for his/her design. The stability graph should also be used with caution, when it is applied to narrow vein orebodies since no version of the graphs account for orebody thickness in the definitions of the stability states.

## 1. Introduction

The stability graph was introduced about three decades ago for bulk mining of orebodies below 1000-m depth by Mathews et al. (1981). The database on which the method was based was limited, consisting of only 26 case histories from 3 mines. For this reason its adoption by the mining industry was slow for lack of confidence in its performance as a design method. The stability graph method is the primary method for open stope design. Potvin (1988) expanded the original database to 175 case histories from 34 mines, and the re-calibrated the stability number factors. Since then, the method has become the primary method for open stope design, and is now widely used in many mines worldwide.

The stability graph is a plot of a stability number *N* against a shape factor *HR* as defined in Equations (1) and (3) respectively, and shown in Fig. 1.

$$N' = (Q')(A)(B)(C) \tag{1}$$

Where *Q'* is defined as:

$$Q' = \left(\frac{RQD}{J_n}\right)\left(\frac{J_r}{J_a}\right) \tag{2}$$

*RQD* is the rock quality designation, $J_n$ is the joint set number, $J_r$ is the joint roughness number, and $J_a$ is the joint alteration number. In equation (1) *A*, *B* and *C* are defined as the stress factor, joint defect orientation factor, and gravity factor respectively. The stress factor *A*, accounts for the effects of induced stresses (Fig. 2a) and varies from 0.1 for high compressive stresses to 1 for relaxed conditions (including tension), with intermediate situations between the two extremes. The *B* factor is defined as the joint defect factor, and is based on the intuition that shallow dipping joints are more likely to cause instability than steeply dipping joints. In other words, shallow dipping joints are more likely to be intersected by newly induced fractures caused by tensile stress conditions or blasting (Fig.

2b). The gravity factor *C*, accounts for the mode of failure which may be in the form of gravity fall, sliding or slabbing. Factors *A*, *B* and *C* are discussed in further detail later in the paper.

**Figure 1. The standard stability graph (Nickson, 1992).**

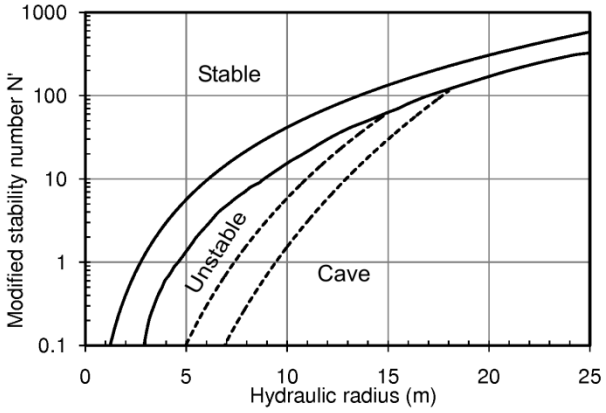


**Figure 1. The standard stability graph (Nickson, 1992)**.

The stope surface shape factor *S* or hydraulic radius *HR* is defined as:

$$HR = \frac{Area}{Perimeter} \tag{3}$$

In the stability graph method, the stability of each stope surface is assessed independently.

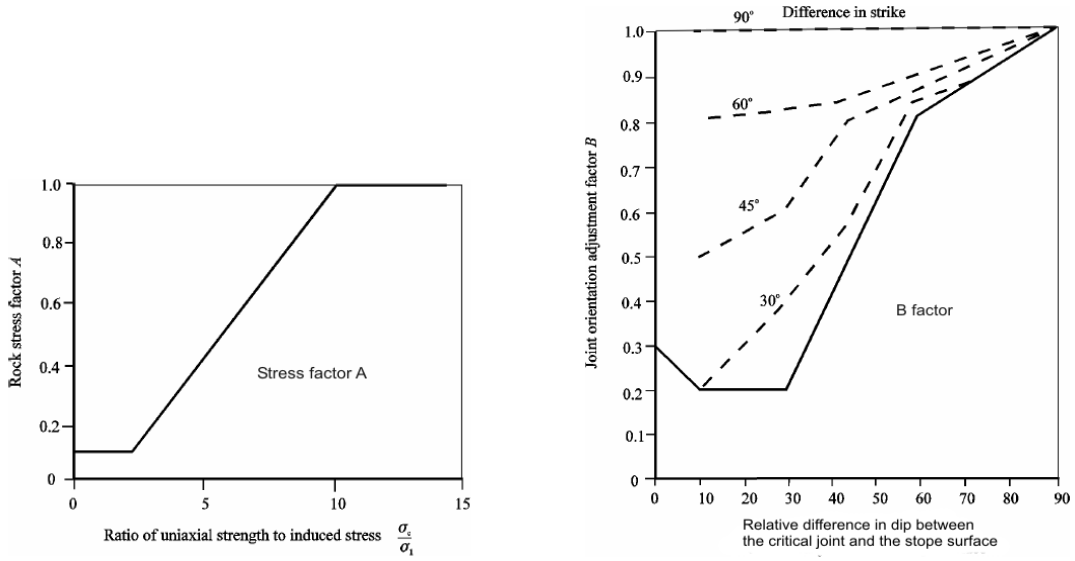


**Figures 2a and 2b. Charts for the determination of the stability graph factors A, B, and C (Mathews et al., 1981): (a) Stress factor and (b) Joint orientation factor.**

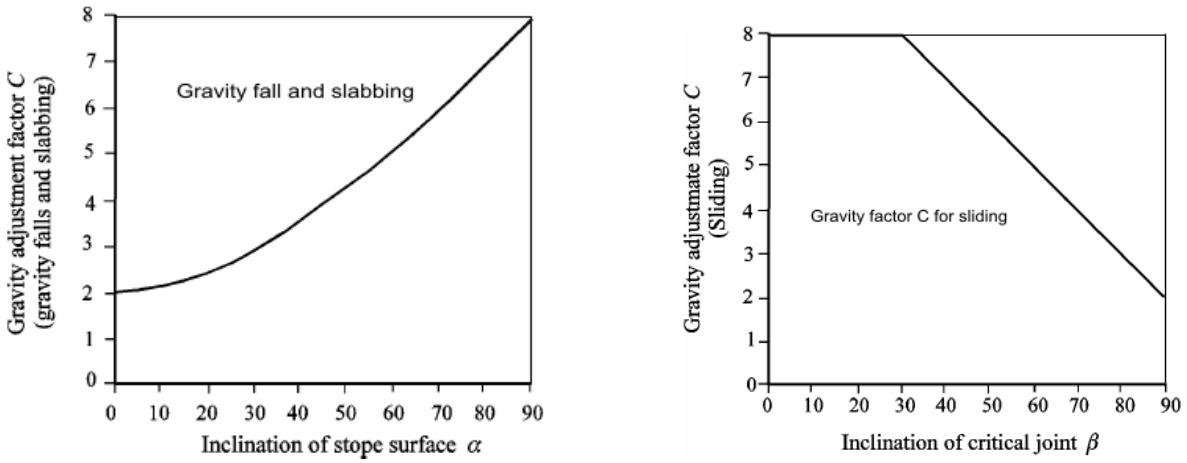


**Figures 2c and d. Charts for the determination of the stability graph factors A, B, and C (Mathews et al., 1981): (c) Gravity factor for wedge fall and (d) Gravity factor for sliding failure.**

The conventional stability graph is divided into three zones: Stable, unstable (or transition zone) and cave. These zones are used to predict the potential stability states of the stope surfaces. Stewart and Forsyth (1995) reviewed the Mathews method for open stope design, and argued that the method was not intended to be rigorous as some authors have tried to imply in their publications. They argued that additional data proved the initial hypothesis of the stability graph method was reasonably good, and that Potvin's (1988) modifications could give the misconception that the stability graph method was rigorous. Subsequently, Trueman et al. (2000), Mawdesley et al. (2001), and Trueman and Mawdesley (2003) used the Mathews et al. (1981) original stability number factors to calculate stability numbers in the expanded stability graph database.

In the conventional stability graph stope surface stability can only be described qualitatively as stable, unstable and cave. This is sufficient for stope sizing and support estimation, but less useful in the estimation of quantified dilution levels. Clark and Pakalnis (1997) introduced the concept of equivalent linear overbreak / slough (ELOS) in the stability graph. ELOS quantifies how much unplanned dilution a stope surface plotted on the stability graph is likely to generate.

## 2. Problem definition and objectives

Several developments have taken place since the introduction of the stability graph in 1981, all aimed at improving its reliability in predicting open stope performance. The most significant limitations identified to date in the stability graph are:

- The sliding failure modes in footwalls are poorly represented by the gravity factor *C*,
- The stress factor *A* does not account for instabilities caused by tension,
- Complex stope geometries are often oversimplified,
- Poor blasting effects are usually ignored,
- Fill surface stability is not accounted for when these form some of the stope surfaces,
- Stand-up time is not considered,
- Effects of faults were not considered, and
- Subjectivity in defining the stability graph zones.

In the past 29 years efforts by various researchers have been focused on eliminating the effects of some of these limitations. The most significant developments are chronicled in Table 1. Some authors (Stewart and Forsyth, 1995; Trueman et al., 2000; Bawden et al., 1989) prefer to use the original stability graph factors by Mathews et al. (1981), while a majority of users of the stability graph in industry use the modified stability graph factors.

The biggest deficiency identified by mine operators using the stability graph was its inability to account for nearby discrete geological structures such as faults and shear zones. Suorineni (1998) critically reviewed case histories from mines in Canada, Australia and Ghana, and developed a fault factor *F* for incorporation into the stability graph method.

Hutchinson and Diederichs (1996) suggest that individual mines develop their own stability graphs calibrated to suit their mining environments. While this is a welcome idea in the interpretation of empirical data there is much to gain in unifying the stability graph zones for general applications. The size and quality of an empirical database dictates the reliability of its predictions. This is demonstrated by the work of Mawdesley et al. (2001) and Trueman and Mawdesley (2003) as shown in Fig. 3.

**Table 1. Chronology of modifications to the stability graph**

| Period | Developments |
|---|---|
| 1980 - 1985 | 1. Introduction of stability graph (Mathews et al.,1981) – 26 case histories |
| 1985 - 1990 | 1. Calibration of stability graph factors and zones (Potvin, 1988) – 175 cases |
| 1990 - 1995 | 1. Tentative cablebolt support line (Potvin and Milne, 1992)<br>2. Re-definition of unstable/cave (supportable transition boundary – cablebolt support line) (Nickson, 1992)<br>3. First partial statistical definition of stable/unstable zone (Nickson, 1992)<br>4. Proposed dilution lines added to stability graph (Scoble and Moss, 1994) |
| 1995 - 2000 | 1. Re-definition of the transition zones (Stewart and Forsyth, 1995)<br>2. Modified gravity factor for sliding failure (Hadjigeorgiou et al., 1995)<br>3. Second partial statistical definition of stable/unstable zones (Hadjigeorgiou et al. 1995)<br>4. Introduction of radius factor *RF* (Milne et al., 1996)<br>5. Calibration of proposed dilution lines *ELOS* (Clark and Pakalnis, 1997)<br>6. Modified gravity factor for footwalls with shallow dips <70° (Clark and Pakalnis, 1997)<br>7. Proposed volumetric index (Germain and Hadgigeorgiou, 1998)<br>8. First complete statistical analysis of stability graph using Baysian likelihood statistic (Suorineni, 1998)<br>9. Introduction of fault factor (Suorineni, 1998; Suorineni et al., 1999b)<br>10. Modified stress factor to include tension and stress-dependent transition zones (Diederichs and Kaiser, 1999) |
| 2000 - 2005 | 1. Expanded database to about 400 cases and modified stability graph zones from Australian database (Truman et al., 2000; Mawdesley et al., 2001)<br>2. Second complete statistical analysis using logistic regression – 483 case histories (Trueman and Mawdesley, 2003)<br>3. Time-dependent stability graph (Suorineni et al., 2001) |
| 2005-to date | 1. Numerical modeling to validate the *B*-factor (Bewick and Kaiser, 2009) |

In Fig. 3, dashed lines show the boundaries of the stability graph defined by Mawdesley et al. (2001) based initially on 400 case histories. When the case histories increased to 483, the boundaries shown in continuous lines were defined. Trueman and Mawdesley (2003) note that with addition of more data statistical distinction between failure and major failure was not as distinct as the boundaries between stable and failure and major failure and caving. Hence, they considered the 2003 boundaries based on the 483 case histories as more reliable.

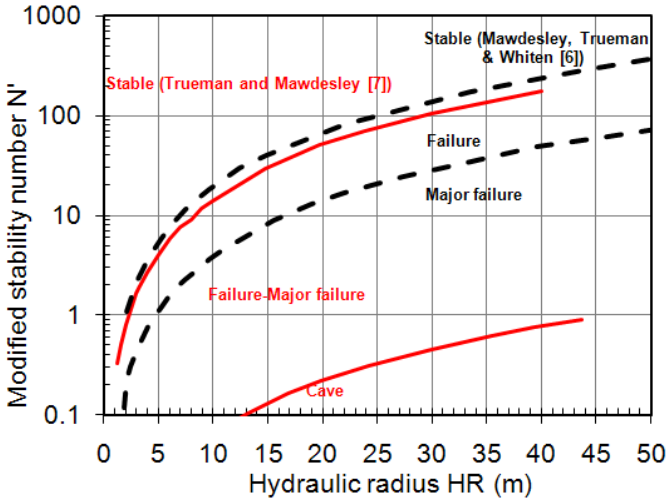


**Figure 3. Effect of data quantity and reliability of empirical methods (Boundaries replotted from Mawdesley et al. (Mawdesley et al., 2001), and Trueman and Mawdesley, 2003).**

The use of different definitions of the stability number factors, and different transition zones have resulted in incomparable data with the following potential problems on the use and further improvement of the stability graph:

- The data bases cannot be combined to further improve the confidence and reliability of the method. Data of different characteristics should not be used in the same database.
- Mixing data computed from different definitions of the stability graph factors in a single database leads to spurious conclusions in design.
- The use of different transition zones in the stability graph prevents experiences gained from one site from being used at another, and undermines the fundamental basis of empirical design, which is the accumulation of expert knowledge for use in similar conditions.
- The existence of different stability graph zones means that the potential stability state of a stope surface will vary depending on which version of stability graph is used. This is a source of confusion for inexperienced users of the stability graph, and practitioners who are unaware of its various developments.

Different types of stability graphs have also emerged in the literature to add to the confusion in the use of the method. These include the original stability graph (here termed "conventional stability graph" or "modified conventional stability graph") for stope size

dimensioning, the equivalent linear overbreak / slough (ELOS) stability graph (Clark and Pakalnis, 1997), the cablebolt design stability graph (Hutchinson and Diederichs, 1996), risk-based stability graphs (Mawdesley et al., 2001; Suorineni et al., 2001) and time-dependent stability graph (Suorineni et al., 2001). The problem with so many types of stability graphs is that no guidelines exist as to when one type should be preferred over others.

Recent experiences (Suorineni, 1998; Stewart and Trueman, 2003) in the application of the stability graph to narrow vein mining show that the conventional stability graph approach does not work for narrow vein mines. Geologically, a vein is defined as a fault or fracture in-filled with mineral material and generally associated with tensional, shear and or dip-slip related deformation (Dominy et al., 1999). However, in mining or economic geology there is no unique definition of a narrow vein deposit, or mine. The literature review shows that the definition of a narrow vein deposit is regional-, national- and or author-dependent. In Sweden, a narrow vein orebody is defined as an orebody with thickness less than or equal to 4 m (Finkel et al., 1987, 2001). In Britain, Brewis (1995a, b) defines narrow veins as mineral deposits which are typically no more than 2 to 3 m wide, and are for most part steeply dipping. Dominy et al. (1999) and Dominy and Camm (1996) (UK and Australia) consider 3 to 6 m wide orebodies as narrow veins. In Canada the definition of a narrow vein ranges from orebodies with widths of less than 2 m (Lizotte, 1993) to orebodies with widths of 10 m as in Nicholas (1981) in the UBC mining method selection procedure. The Canada Centre for Mineral and Energy Technology (CANMET) (1999) defines a narrow vein deposit as one with thickness less than or equal to 5 m. Thus, in Canada and UK, the definition of a narrow vein deposit is author-dependent. Dirige (1996) in the Philippines defines narrow veins as orebodies with widths less than 2 m.

In the author's opinion, the definition of a narrow vein orebody in the mining context should be both geometry and technology dependent. It is difficult to mechanize mining of orebodies with widths less than 2 m without causing excessive dilution. It is also difficult to mine veins less than 0.1 m thick manually without causing unacceptable dilution and severe discomfort to miners. Based on the above discussion, in this paper a narrow vein orebody is defined as one with thickness less than or equal to 2 m.

The objectives of this paper are to:

- Bring to light the confusion created by researchers in the arbitrary choice of the Mathews et al. (1981) set of stability number factors and those suggested by Potvin (1988) and vice versa, and to provide guidelines.
- Bring to light the confusion created by researchers by the different transition zones between stope stability states (stable/failure, failure/cave; stable/failure-major failure, failure-major failure/cave etc.) and to provide guidelines.
- Create awareness among users of the various types of stability graphs and provide proper guidance on when each should be used.
- Caution users on application of the stability graph methods to open stope design in narrow vein orebodies.
- Give directions for further improvements to the stability graph; and
- To bring the scattered stability graph knowledge to a common source for easy understanding and reference.

The overall goal is to improve on the use of the stability graph so that experiences gained in one mine can be used as guidance in another, and to suggest areas for further research to improve the reliability of the stability graph method for open stope design.

## 3. Modifications to the stability number *N*

### *3.1 Stability number factors*

The calibrated stability graph factors (Fig. 2) resulted in a modified stability number N-prime *N'*. Experience shows that factors *A* and *C* still need to be re-defined. To date there are two schools of thought when it comes to choice of the factors for calculating the stability number *N (or N')*. One group favours the original stability graph factors by Mathews et al. (1981), while another is in favour of the modified factors by Potvin (1988). Based on the experience that the reliability of empirical methods depends on the size and quality of the database it is logical that the Potvin calibrated factors should be more reliable. These factors are discussed in the following sections, and later in the paper.

#### *3.1.1. Stress factor*

According to Equation (1), lower values of factor *A* reduces the stability number *N*. As factor *A*, increases to 1 the stability number increases to a maximum at *A* equals 1, presumably in moderate stress conditions. At the same time Mathews et al. (1981), and more recently

Stewart and Forsyth (1995) state that the induced stresses be set to zero when tensile, and factor *A* set to 1 since the quotient of the intact rock uniaxial compressive strength over induced stress becomes infinity (greater than 10). Thus, stress factor *A* for moderate and induced tensile stress conditions are equal. The implication is that for stope surfaces in moderate stress conditions and tension, stability is maximum. The authors later state that for *A*=1 for tension, failure is structurally controlled and gravity driven. Hence, the role of factor A is not only confusing but mechanistically false since blocky rock masses are known to be unstable in tension (Barton et al., 1974; Bieniawski, 1988; Goodman, 1989), and more stable in moderate stress conditions. This is amply demonstrated in the case of the voussoir beam (Evans, 1941; Sofianos, 1996). Intuitively, moderate stress conditions should give a stress factor *A* greater than 1, rather than have no effect as is the case when *A*=1 for such conditions. The stress reduction factor *SRF* concept (Barton et al., 1974) which is approximately an inverse of the stress factor *A* (Hoek and Brown, 1980) reflects this proposition. Also, Bieniawski (1988) suggests that for moderate stress conditions a rating of 1.2 should be applied in *RMR* to reflect increased stability.

Stress is often viewed as having only adverse effects on excavation stability, yet moderate stresses ($0.1<\sigma_1/UCS<0.4$) have positive impact on excavation stability. In this stress range, stress neither fractures intact rock nor allows structurally controlled unravelling. In blocky rock masses moderate stresses clamp wedges to keep them in place. For normal wedge sizes, Suorineni et al. (1999a) determined that the critical range of clamping stresses is 0.01 to 0.2 MPa, below which structural failure will occur in blocky rock masses.

The gravity factor is only effective in blocky rock masses with zero tensile strength or in rock masses where stresses (compressive or tensile) are high enough to destroy rock bridges. Thus, the gravity factor *C* should not be independent of the stress factor *A*, as is currently the case. Current assumption is that all rock masses are discontinuous with no tensile strength. Sprott et al. (1999) argue that following the brittle Hoek-Brown failure criterion (Martin, 1997) logic rock mass damage increases with depth even without excavation considering that the farfield deviator stress increases linearly with depth. They defined an extra stress deviator factor (D) (Equation 4) to account for existing rock mass damage prior to excavation. The damage factor (D) ranges from 0.1 to 1. It is used to adjust $RQD/J_n$ in equation (2) since the damage results in fractures to reduce *RQD* and increase $J_n$.

$$D = \left(\sigma_1^i - \sigma_3^i\right) - \left(\sigma_1^f - \sigma_3^f\right) \quad (4)$$

Where $\sigma_1$and $\sigma_3$ are major and minor principal stresses respectively and superscripts *i* and *f* refer to induced and farfield stresses respectively.

To account for complete relaxation more effectively in the stability graph Diederichs and Kaiser (1999) suggest a tension component to the stress factor chart (Fig. 4a). The tension chart however, remains to be calibrated or fully tested. It does not account for partial relaxation or moderate stresses in blocky rock masses. Further research is needed in this direction in order to improve the reliability of the stability graph in these ground conditions, taking into account the domains of effectiveness of the gravity factor as discussed earlier.

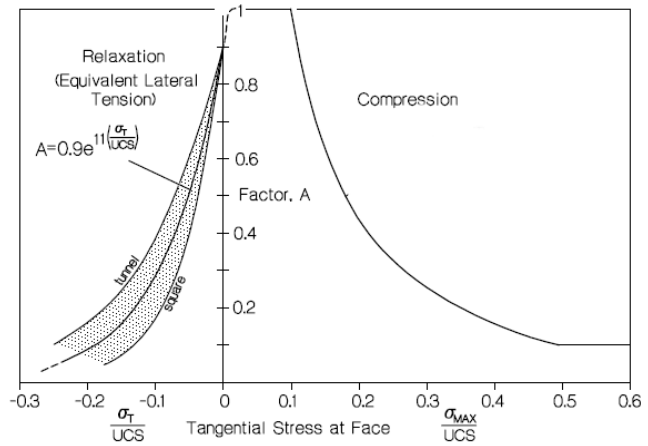


**Figure 4a**

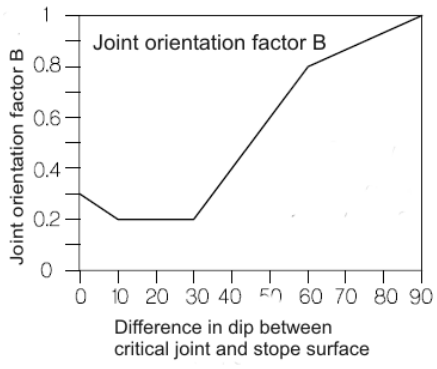


**Figure 4b**

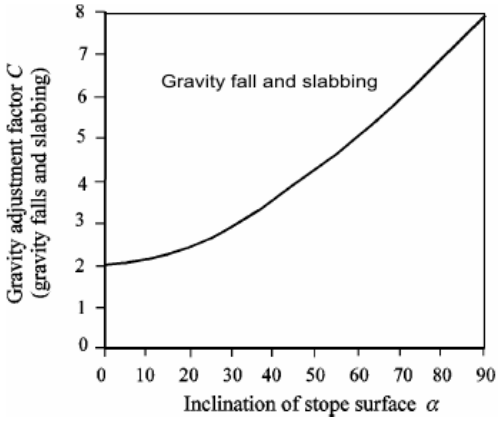


**Figures 4c**

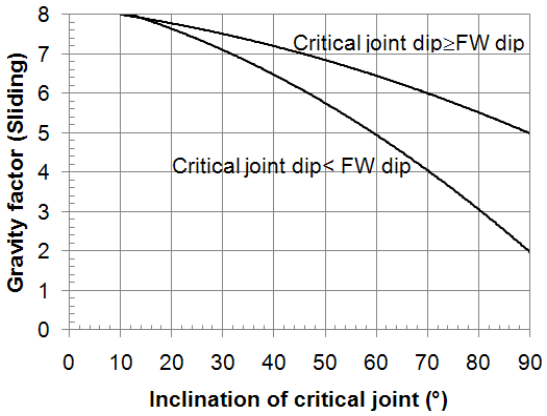


**Figures 4d**

**Figures 4a to 4d. Calibrated and modified stability graph factors (a) includes A-factor for tension (Diederichs and Kaiser, 1999), (b) B-factor (Potvin, 1988), (c) Gravity factor for wedge fall (Mathews et al., 1981) and (d) Gravity factor for sliding failure (Hadjigeorgiou et al., 1995).**

### *3.1.2. Joint defect factor*

Bewick and Kaiser (2009) used numerical modelling to show that different B factors are required for the different stope surfaces (Fig. 5). This observation is in agreement with the work of Suorineni (1998) on the effects of faults on open stope stability. The latter suggested that the effect of a structure on open stope surface stability is dependent on both the stope surface, and the location of the structure on the stope surface. Bewick (2009) concluded that the *B* factor is also affected by joint confinement and interblock rock mass strength.

### *3.1.3. Gravity factor*

There still does not exist, an acceptable chart for determining the gravity factor for stope footwalls. While the gravity factor for footwalls may not be routinely used by practitioners, because of the relatively stable nature of open stope footwalls, it is still important to have an effective gravity factor for the assessment of open stope footwalls. In its current form, the gravity factor does not work for footwalls, and even though its current form implies it is applicable to hangingwalls with dips ranging from 0˚ to 90˚, the database contains only hangingwalls with dips in the range of 60˚ to 80˚ approximately. Hence, *C* should be applied with caution when dealing with hangingwalls with dips outside this range.

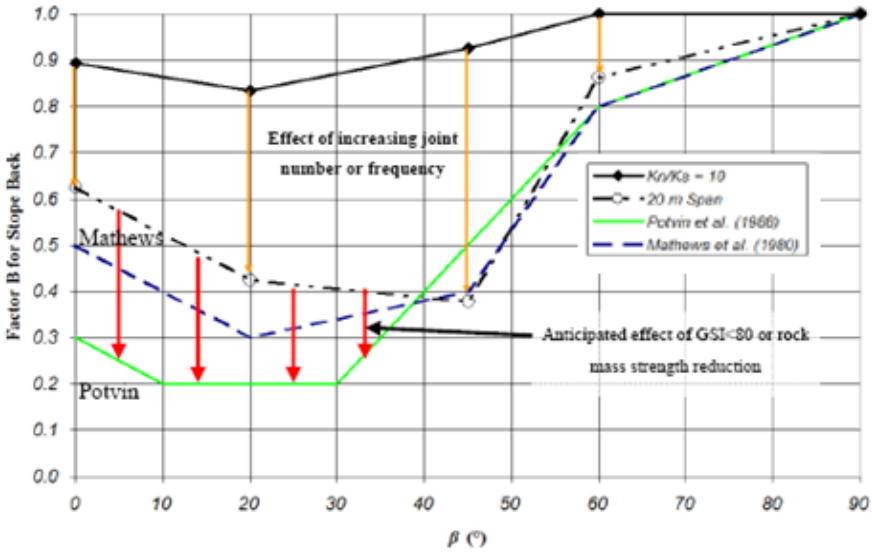


**Figure 5a. B-factor curves derived from numerical modelling for given conditions for stope back and hangingwall (Bewick, 2008): Typically numerically derived Factor B curve for the stope back. Joint spacing 2m, $K_n/K_s$ = 10, $k_o$ = 1, and $\varphi$ = 40°. Arrows show effect of joint spacing due to stope back span increasing from 10 m to 20 m (from 5 to 10 structures intercepting stope back).**

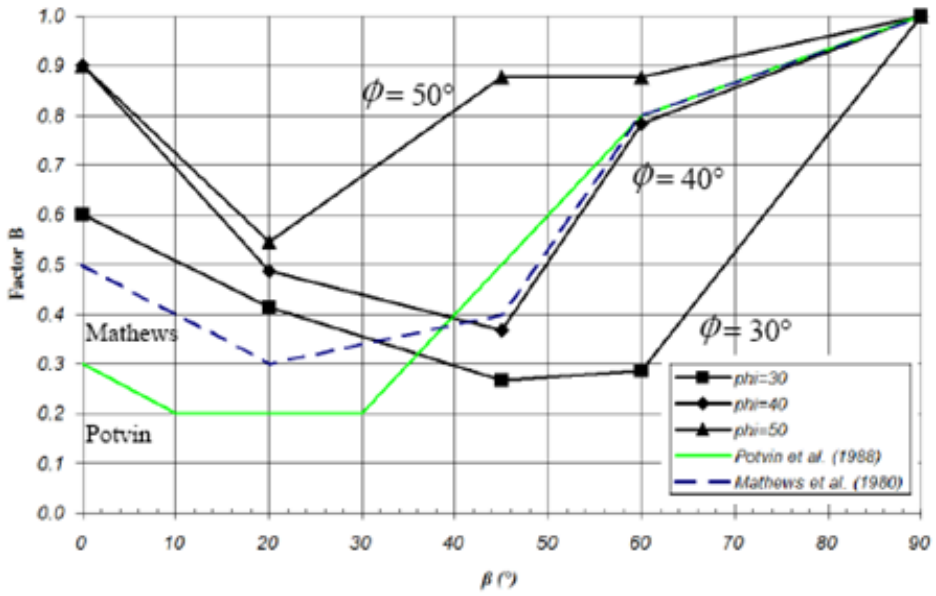


**Figure 5b. B-factor curves derived from numerical modelling for given conditions for stope back and hangingwall (Bewick, 2008): Effect of joint friction ($\varphi$ °) on stope hanging wall stability (ko = 1, joint spacing of 2 m, and $K_n/K_s$ = 10).**

The difficulty to date is defining a gravity factor for low dipping (dips<70°) footwalls. Several authors (Potvin, 1988; Hadjigeorgiou et al., 1995; Clark and Pakalnis, 1997) have found through experience that the original gravity factor (Fig. 2c) as defined by Mathews et al. (1981) does not apply to footwalls with dips less than 70°. It does not also account for sliding failure. These factors are currently determined from Figs. 4c and 4d or from the original Mathews et al. chart (Fig. 2c).

In the absence of an acceptable chart for *C*, Clark and Pakalnis (1997) used a gravity factor of 8 for all stope footwalls dipping less than 70°. They suggest *C* values above 8 for lower dipping footwalls. The most constructive work on the gravity factor to date, is the work by Hadjigeorgiou et al. (1995) shown in Fig. 4d for sliding failure.

Further work is required to establish an association between the stress and gravity factors. The lack of association of factors *C* and *A* is the likely source of the difficulty in establishing an acceptable *C* factor, and the misclassification of some stope stability states. Misclassification of stope surfaces could also result when stope surface stabilities are not deduced from cavity monitoring surveys but by visual inspection. Based on current knowledge, in this paper Fig. 4d is recommended for sliding mode failures in stope walls, while Fig. 4c should be used for gravity fall modes of failure.

### *3.2. Additional factors affecting open stope stability*

#### *3.2.1. Fault factor F*

The Q-system (Barton et al., 1974) does not adequately account for the presence of faults. Hence, *Q'* in Equation (1) does not account for faults. The stability of open stopes is frequently affected by the presence of nearby faults. In many mines that utilize open stope mining methods, stope walls assessed as stable using the conventional stability graph often cave when faults are present. Sloughage of stope walls is a major concern in mines because of ore dilution, ore loss and increased production cost. Suorineni et al. (1999b) developed a fault factor for incorporation into the stability graph method for open stope design (5).

$$N'_f = (Q')(A)(B)(C)(F) \quad (5)$$

where $N'_f$ is the modified stability number that accounts for the presence of nearby faults. Fig. 6 gives charts for determining the fault factor *F*. For non-intersecting faults, the fault distances are normalized, by dividing by the inclined stope height. Faults tend to have the greatest influence on stope stability when the angle between fault and stope surface is about 20º to 30º. Faults that are nearly perpendicular to the stope wall have little effect.

#### *3.2.2. Time effects*

Stope life spans are important in design since the best ore extraction method is that which enables completion of mucking and filling just in time before the stope collapses. Open stopes are normally designed to last one to six months from first blast to depletion. In extreme cases stope life spans could be a year or more. Stopes are either backfilled immediately following depletion, or fill may be delayed or could be completely ignored. Time effects on stability, and the consequences on ore dilution primarily dictate the choice of whether to backfill, when to backfill and not to backfill. In most cases, scheduled stope life spans are exceeded because of unexpected delays in the mining cycle. Fig. 7 shows that the effect of time on open stope stability can be significant. Fig. 7a shows the propagation of open stope sloughage with time and Fig. 7b shows increasing dilution with time in a stope hangingwall at Detour Lake Mine.

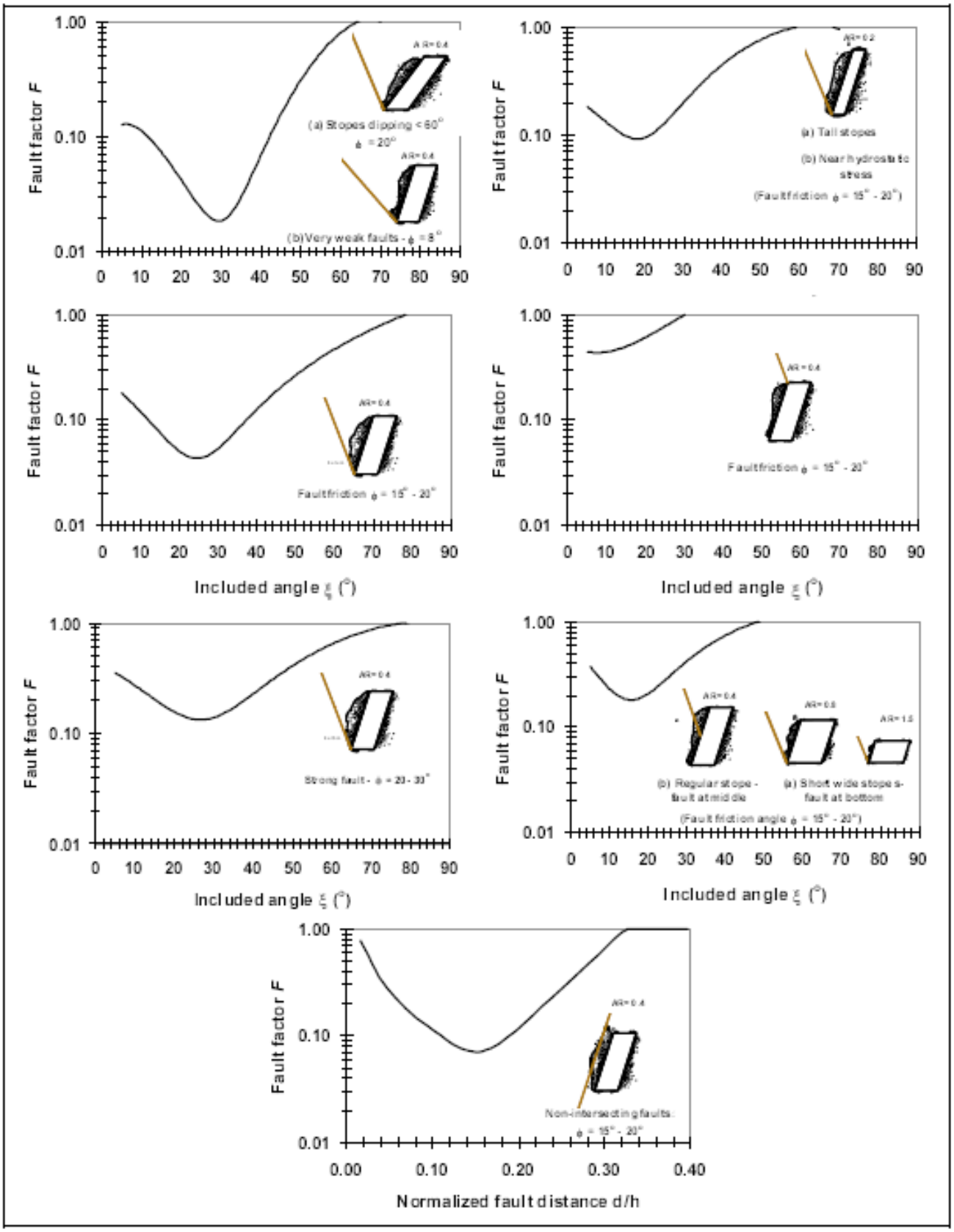


**Figure 6. Charts for determining fault factor for various conditions (Suorineni et al., 1999b).**

Notice that the footwall is relatively stable. Tannant and Diederichs (1997) recognized the time-dependent behaviour of stope wall stability at Kidd Mine and made adjustments to the rockmass quality *Q'* to account for time (Table 2). Equation (6) was then applied to determine the correct stability number *N** to account for time.

$$N^* = (Q')(A)(B)(C)(T) \qquad (6)$$

where *T* is time correction factor.

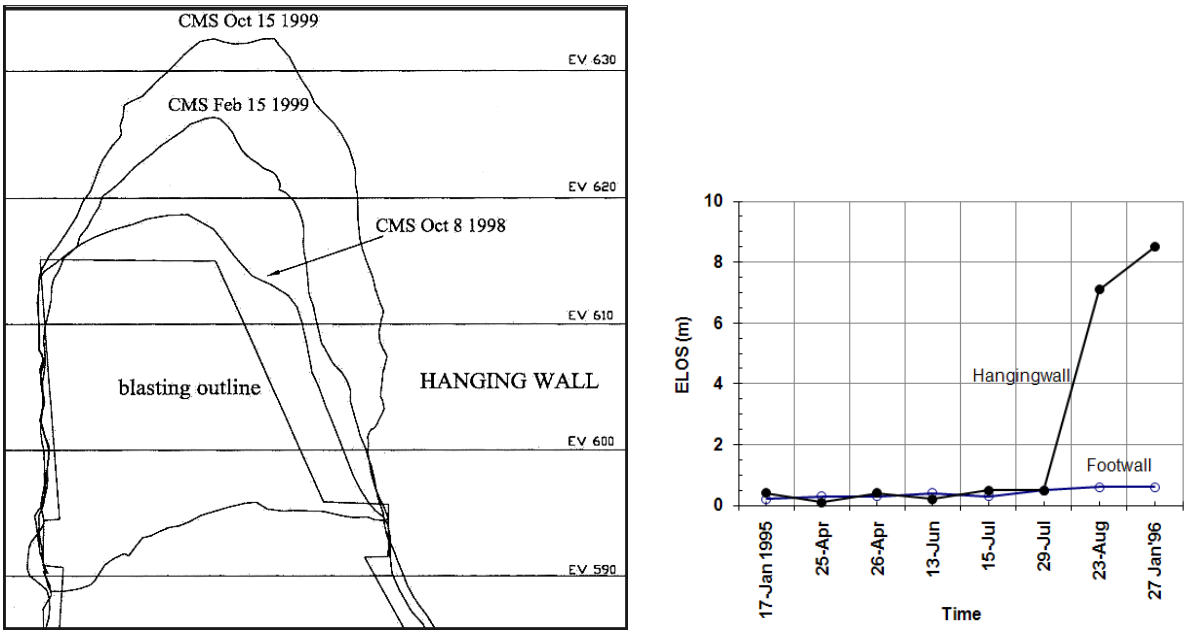


**Figures 7a and 7b. Time effect on open stope stability. (a) Stope back sloughage with time – Ruttan Mine (Ran, 2002). (b) Increasing dilution with time at Detour Lake Mine (data from Dunne and Pakalnis, 1996).**

**Table 2. Time correction factors (Tannant and Diederichs, 1997)**

| Wall exposure time | Time factor *T* | |
|---|---|---|
| | ***Q'*>10** | ***Q'*<10** |
| <3 months | 1 | 0.8 |
| 3 to 5 months | 0.8 | 0.5 |
| 5 to 12 months | 0.5 | 0.3 |
| >12 | 0.3 | 0.2 |

The stand-up time chart by Bieniawski (1973) linking excavation span and rock mass quality to excavation exposure time supports time effects on excavation stability. Laubscher (1990) modified *RMR* to include time effects among others for mining. These evidences are supported by industry practice where emphasis is often placed on timely backfilling of open stopes to curb dilution. It is thus important to have a stability graph that accounts for time.

When time-dependent stope wall failure data are superimposed on the modified stability graph, the stable-unstable boundary fit a 1-year or more stand-up time boundary. Beyond this limit, stope sizes are more sensitive to time (Fig. 8).

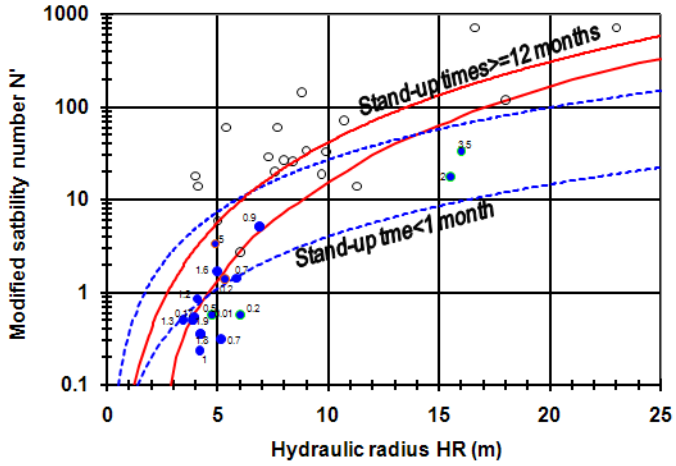


**Figure 8. Accounting for time in the stability graph: Numbers are stope stand-up times in months (Suorineni et al. 2001).**

The excavation support ratio *ESR* (Barton et al., 1973) depends on the excavation life span and function (Table 3). Mathews et al. (1981) used an *ESR* of 1.6 for permanent mine openings in developing the gravity factor *C* for open stopes which are, in fact, temporary mine openings. Consequently, the original gravity factor *C* is conservative.

Because *ESR* accounts for time, appropriate values of *ESR* can be used in defining *C* to account for stope life spans. Suorineni (1998) suggested that effects of time can be accounted for in the stability graph by using the appropriate *ESR* value from Table 3 in Equation (7) (Fig. 9) to determine *C* to account for time effects in the stability graph. Note that the maximum value of *C* is *ESR* dependent.

$$C = 5ESR - (5ESR - 2)\cos\theta \qquad (7)$$

where $\theta$ is the dip of the stope surface.

### *3.2.3. Blasting effects*

Effect of blasting is not yet accounted for in the stability graph. In rock mass characterization ISRM (1981) recommends that only natural discontinuities be considered. Therefore, in Equation (1) blast-induced damage is not accounted for in the modified *Q'*. Suorineni et al. (2008) argue that excavation induced damage in rock masses should be taken into account in estimating rock mass quality for support selection. This argument is supported by Løset

(1997) and Hoek et al. (2002). By including newly created fractures in the estimation of rock mass quality *Q'*, the effect of blasting will be explicitly and more appropriately accounted for in the stability graph. Clark and Pakalnis (1997) account for blasting effect in ELOS by adding approximately 0.5 m to the values where appropriate.

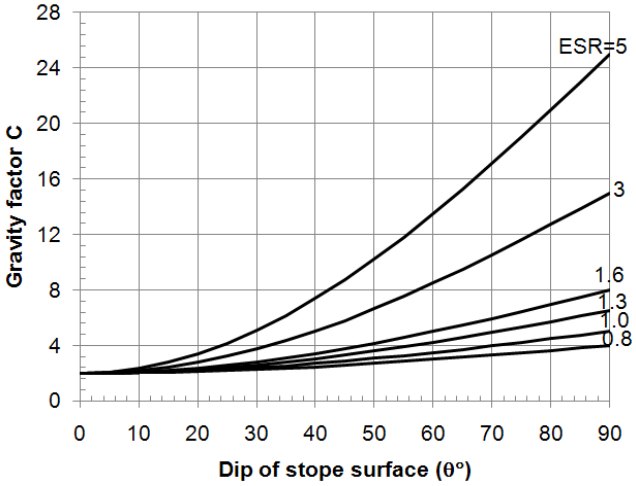


**Figure 9. *C* factor chart for various stope life spans.**

**Table 3 *ESR* for underground excavations (Løset, 1997)**

| Excavation category | Excavation type | ESR |
|---|---|---|
| A | Temporary mine openings | 3-5 |
| B | Circular shafts | 2.5 |
| | Rectangular shafts | 2.0 |
| C | Permanent mine openings, water tunnels for hydropower , pilot tunnels drifts and headings for large openings | 1.6 |
| D | Storage rooms, water treatment plants, minor road and railway tunnels, surge chambers, access tunnels, etc. | 1.3 |
| E | Power stations, major railway tunnels, civil defense chambers, portals, intersections, etc. | 1.0 |
| F | Underground nuclear power stations, railway stations, sports and public facilities, factories, etc | 0.8 |

This approach is likely to under or overestimate blast damage depending on blasting practice and skill of personnel.

### *3.3. Choice of stability graph number factors*

A review of the literature reveals that the selection of which stress factor *A*, joint defect factor *B*, and gravity factor *C* to use in the determination of *N* is dependent on the author's preference. Stewart and Forsyth (1995), Trueman et al. (2000) and Mawdesley et al. (2001)

all argue that modifications to the original stability graph factors and subsequent contributions do not make any significant difference, and therefore adhere to the original Mathews factors. There is significant difference between Mathews et al. (1981) original stress factor *A*, and Potvin's calibrated *A* factor when $UCS/\sigma_1$ is less than 2. Consider a hypothetical case in which $\sigma_1$ is 250 MPa and *UCS* is 100 MPa. Mathews original stress factor gives the stress factor *A* as zero and 0.1 for modified Potvin stress factor. Also consider a stope hangingwall of dip $70^o$ with a critical joint dip of 80° into the stope. Potential mode of failure is wedge sliding rather than gravity fall. Based on Mathews *C* factor *C*=6, and using Potvin's *C* factor *C*=3. It has to be noted that while Mathews et al. *C* factor is applied to both sliding and gravity falls the Potvin modified *C* factor differentiates between sliding and gravity failure mechanisms, and it is an important contribution in assessing stability of footwalls even though it is found inadequate for footwalls by Clark and Pakalnis (1997). They suggested assigning a $C \geq 8$ depending on the wall dip. Thus, there is difference between the Mathews et al original stability number factors and the modified factors by Potvin.

## 4. Shape factor (HR/S)

Experience with the use of the hydraulic radius *HR* shows it is inadequate in describing the performance of stope surfaces with complex geometries (Germain et al., 1996; Milne and Pakalnis, 1997) and in dealing with vertical and horizontal rectangular stope surfaces Henning and Mitri (2006).

Rectangular hangingwall stope surfaces with different dimensions and orientations can give identical hydraulic radii (e.g. stope height of 15 m and strike length 30 m versus stope height of 20 m and strike length of 20 m both give *HR*=5). The two stope surface orientations have important implications in terms of dilution potential and yet have the same *HR* values.
For complex stope surfaces Milne et al. (2004) introduced a new shape factor called the radius factor *RF* (Equation 8).

$$RF = \frac{0.5}{\frac{1}{n}\sum_{\theta=1}^{n}\frac{1}{r_\theta}} \tag{8}$$

where $r_\theta$ is distance from stope surface centre to the abutments at angle $\theta$, and *n* is the number of rays measured to the surface edge.

An important distinction should be drawn between application of the stability graph to planning of stope sizes and the actual stope geometries following extraction. At the planning stages only simple planar stope surface geometries can be used. These simple planar stope geometries can become complex following excavation depending on drilling accuracy and blasting practice. Thus, while a planned stope surface may indicate stability the complexity of the same surface might render it unstable following excavation. RF is thus more practical in assessing stope surface stability if actual stope surface geometries can be predicted. Milne et al. (1996) state that there is little difference between *HR* and *RF*, for openings with length to span ratios less than 10:1. As explained earlier, even within this span to length ratio, stope surface geometries may still be complex. Hence, it is more realistic to use *RF* in defining stope surfaces in the stability graph.

## 5. The transition zones

### *5.1. "Eyeballed" transition zones*

In both the original and modified stability graphs, the demarcations between different clusters of stope stability states were "eyeballed" (Fig. 10 and Fig. 11). Fig. 10 was based on only 26 case histories and divided into three zones: potentially stable, potentially unstable and potentially caving.

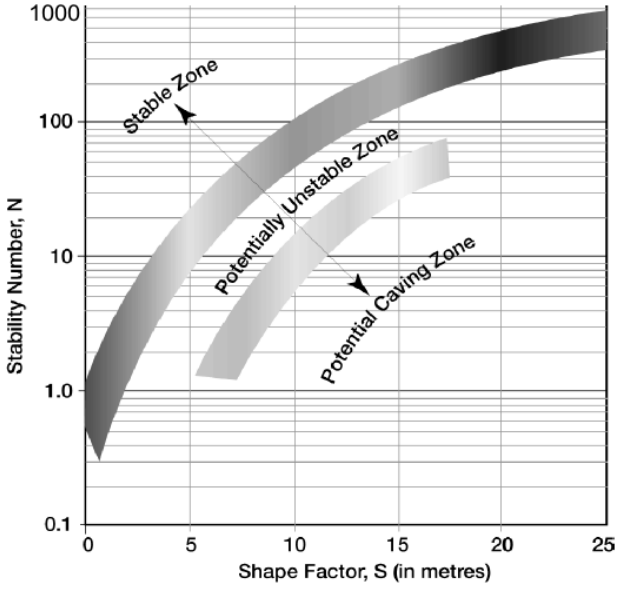


**Figure 10. Original stability graph transition zones (Mathews et al., 1981).**

Fig. 11 was based on 175 case histories and divided into two zones: stable and unstable. Nickson (1992) increased the number of case histories by 59 and also redefined the stability graph boundaries by "eyeballing" (Fig. 1), into three zones: stable, unstable (stable with

support) and caving. Fig. 1 is referred to as the Potvin-Nickson modified stability graph. Stewart and Forsyth (1995) reviewed the stability graph method and proposed three boundaries by "eyeballing" to give the stability graph four zones: potentially stable, potentially unstable, potential major failure, and potential caving (Fig. 12).

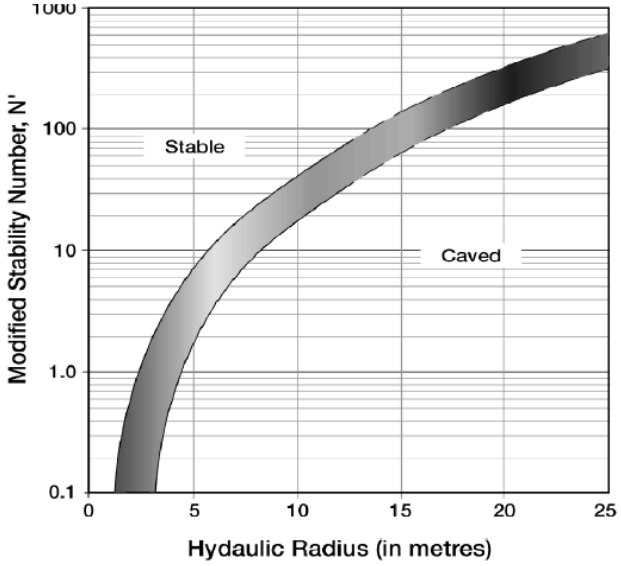


**Figure 11. Modified stability graph (Potvin, 1988).**

Potvin (1988) recognized the defect in "eyeballing" the transition zones, and suggested the use of statistics to define them. The application of statistical methods to define the stability graph zones is discussed in detail in Section 5.2.

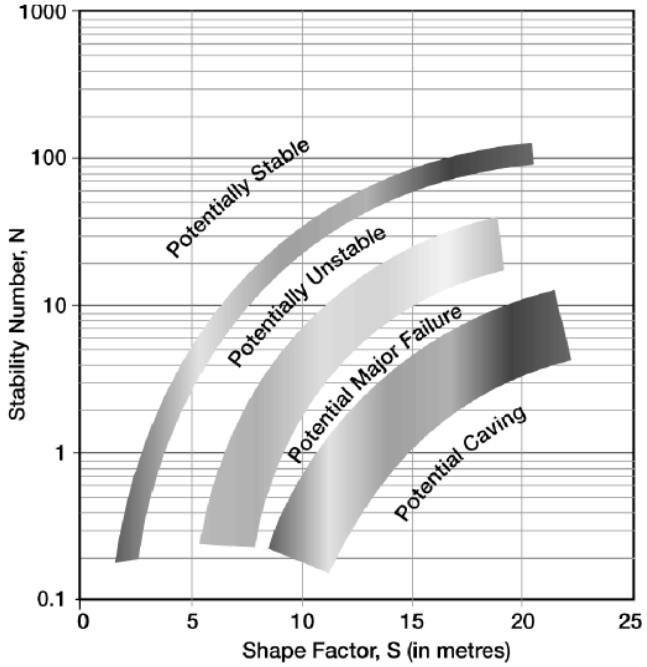


**Figure 12. The stability graph boundaries as defined by Stewart and Forsyth (1995).**

The use of the term "potential" by Mathews et al. (1981) and Stewart and Forsyth (1995) in describing the stability states of stopes is significant. The stability states of points plotted on the stability graph are based on the axiom of stability state likelihood only, and cannot be described or assumed definitive. The purpose of the stability graph is to predict stability states of future stopes from past performance of stopes. Therefore, it is more realistic to describe stability states of points on the stability graph probabilistically rather than definitively.

### *5.2 Application of statistics*

In recent times, refinements to the stability graph have concentrated on the application of statistics to define the stability graph zones, and for interpretation of points on the stability graph. These are discussed in the following sections.

#### *5.2.1 Mahalanobis distance method*

Nickson (1992) and Hadjigeorgiou et al. (1995) independently used discriminant statistics to verify the transition zone between stable and unstable stopes (Fig. 13). They both concluded that the Potvin (1988) "eyeballed" transition zone between stable and failed zones was sufficiently accurate. The statistical transition zones were defined by single curves compared to the eyeballed transition zones which are bands to accommodate uncertainty.

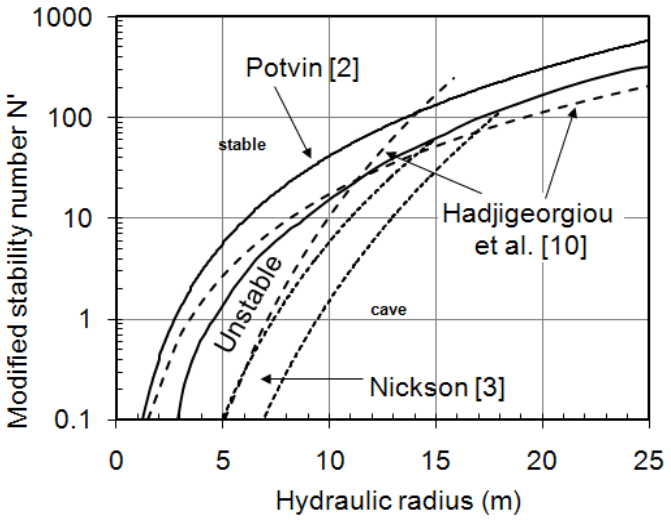


**Figure 13. Stability graph showing the "eyeballed" transition zones and statistically defined zones.**

#### *5.2.2 Likelihood statistic*

Suorineni (1998) used the likelihood statistic to interpret the stability graph. The likelihood statistic was used to:

- Define the stability graph zones,
- Optimize the stability graph boundaries taking into account bias in number of cases in the stability state case histories (i.e. account for misclassification of stope surface stability states) and the associated cost,
- Determine degrees of overlap in the stability graph zones,
- Determine performance prediction errors, and
- Introduce multiple design curves based on likelihood (Equation 9) of a stope surface stability state.

$$HR = 10^{(0.4905 - 2\log\Lambda + 0.3738\log N')} \quad (9)$$

where $\Lambda$ is the likelihood ratio.

Equation (9) was used to develop a stability graph with multiple contours of likelihood of failure (see Section 6.4). This work showed that the Mahalanobis distance method is a special case of the likelihood method, where the likelihood ratio is 1.

*5.2.3 Logistic regression*

Trueman et al. (2000) and Mawdesley et al. (2001) examined the Mathews stability graph method to see how it could be applied to underground mines in Australia. They defined a general transition boundary based on a combination of the Australian and Canadian databases. Fig. 3 shows change in the transition zones with increased data. In the first case, their transition boundary is a single one based on 400 cases histories, essentially dividing the data into stable and failed stopes, while in the second case based on 483 case histories, the graph is divided into stable, failure/major failure and cave. They used the term "cave" in the context of cave mining as opposed to its usage in open stoping nomenclature that implies major stability problems as pointed out by Potvin and Hadjigeorgiou (2001).

The stability zone between stable and caving zones in Fig. 3 as established by the logistic regression method is however too broad, implying a lot of uncertainty in this region. The explanation given by Trueman and Mawdesley (2003) for this wide zone is that the statistical distinction between failure and major failure is less distinct compared to stable-failure and major failure and caving.

### *5.3 Consequences of the different stability graph zones*

Fig. 14 shows a stability graph with the major published stability graph zones, including the *ELOS* contours from Clark and Pakalnis (1997). The stability graph boundaries defined by Mawdesley et al. (2001) and Trueman and Mawdesley (2003) are both included. As expected, the stability graph zones are more database size dependent than on the response of stopes. Another reason for the different stability graph zones is the use of different factors (*A*, *B*, and *C*) for the determination of the stability number *N*. Determination of stope surface stability state without cavity surveys could also lead to stope stability states misclassification and impact the stability zones. Fig. 14 shows the dilemma faced by the inexperienced user of the stability graph with no knowledge of these potential contradictions. The following example illustrates the problem. Points X and Y are stability states of two stope surfaces. According to the Nickson-Potvin transition zones stope surface X will cave, while according to Trueman and co-workers the stope surface is stable. The *ELOS* contour predict this stope surface, will suffer an overbreak of 0.5 m primarily due to blasting, and is therefore stable, in agreement with Mawdesley et al. (2001) and Trueman and Mawdesley (2003).

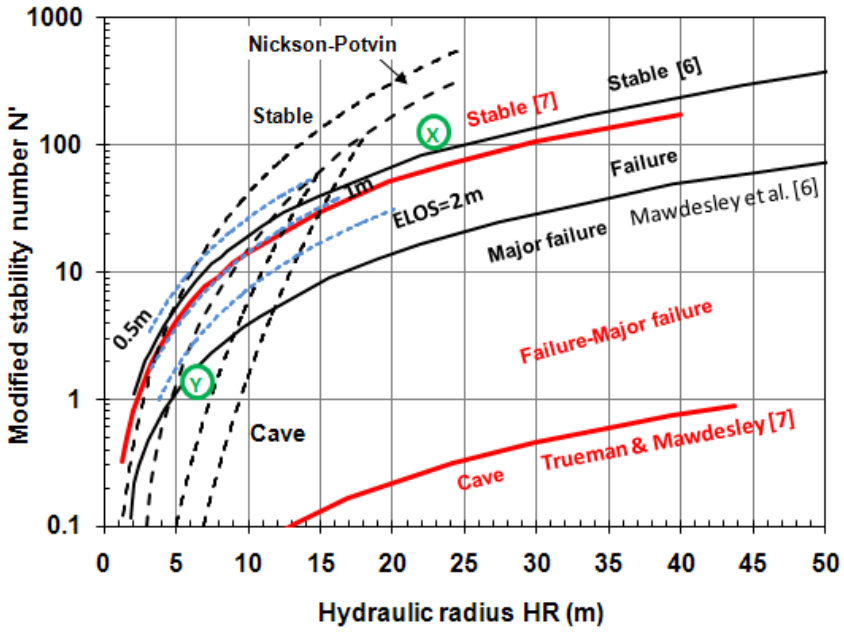


**Figure 14. Stope stability states calculated with different factors plotted on a stability graph with the different transition zones showing that depending on each transition zones the stope stability states are different.**

On the other hand, stope surface Y can be stabilized with support according to Nickson and Potvin, but will suffer failure-major failure according to Mawdesley et al. (2001) and Trueman and Mawdesley (2003). This stope surface will suffer an *ELOS* greater than 2 m that is equivalent to caving (major stability problems) according to Clark and Pakalnis (1997).

What is the appropriate stability state of these stope surfaces (i.e. which stability graph boundaries are correct)?

## 6. Types of stability graph

The stability graph was originally developed to optimize longhole stope dimensions. In this sense, stopes are either potentially stable (no support required), potentially unstable (support required) or potentially cavable (unsupportable). These descriptions are qualitative. Various applications of the stability graph have since evolved. Users of the stability graph need to be aware of these alternative applications, and know when and how to use them. The following are brief introductions of these variations of the stability graph with guidelines to users on which stability graph to use and when.

### *6.1 Stope dimensioning*

Rock mass quality, and stress state dictate the size of open stopes. For a new or operating mine these are the key parameters for planning new non-entry stopes. The conventional stability graph (Fig. 1) is a useful tool for this purpose. In the planning stages, stope sizes and estimated support for stope walls are needed for safe and economic mining strategies. However, by this method no quantitative estimation of dilution can be made as stability assessment is essentially qualitative.

### *6.2. Dilution (ELOS)-based stability graph*

Dilution is a major concern in many mines, and it is just not sufficient to know whether a stope is going to fail or be stable, but more importantly, miners are interested in knowing how much dilution is going to be produced, and whether this dilution is acceptable. Acceptable dilution levels vary from mine to mine, and depend on the type of mineral and mining method.

Pakalnis (1986) published the first dilution-based stability graphs, and gave a comprehensive summary of the various definitions of dilution as practised in Canadian mines. Recent developments in cavity surveys (Miller et al., 1992), and the proposition to superimpose dilution contours on the stability graph (Scoble and Moss, 1994) made it possible to develop a dilution-based stability graph in terms of average depth of failure, the equivalent overbreak slough *ELOS* (Equation 10) (Clark and Pakalnis, 1997; Clark, 1998). The *ELOS* stability graph is shown in Fig. 15.

$$Equivalent\,Linear\,Overbreak/\,Slough = \frac{Volume\,of\;\;slough\;\;from\,stope\,surface}{Stope\,height\,x\,Wall\;strike\,length} \qquad (10)$$

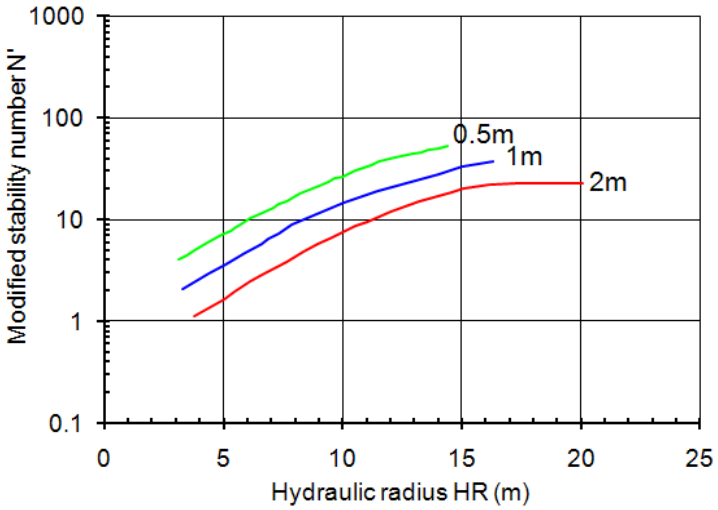


**Figure 15. ELOS stability graph (Clark and Pakalnis, 1997).**

### *6.3. Cablebolt design stability graphs*

Open stopes are non-entry excavations, and are often amenable to deep hangingwall sloughage. For stabilization of open stope hangingwalls and footwalls, remote access is required. The flexibility to cut cablebolts to desired lengths makes them the most suitable support system for these conditions. Diederichs et al. (1999) used the stability graph for detailed cablebolt design where the type of cablebolt, its spacing and length can be selected. Fig. 16 shows the cablebolt design stability graphs. It should be noted that the cablebolt design charts are based on the Potvin-Nickson stability graph transition zone, and always tend to give hangingwall cablebolting pattern of 2.2 m for standard size stopes (Henning, per. comm.).

### *6.4. Risk-based stability graphs*

There are three types of risk-based stability graphs namely: probability-based stability graph (Diederichs and Kaiser, 1999) the Baysian likelihood statistic (Suorineni et al. 2001) and the logistic regression-based (Mawdesley et al., 2001) stability graphs. The advantage of risk-based stability graphs is that depending on the mine acceptable risk of dilution level, they can size their stopes accordingly. These graphs represent the current direction of analysis of the stability graph.

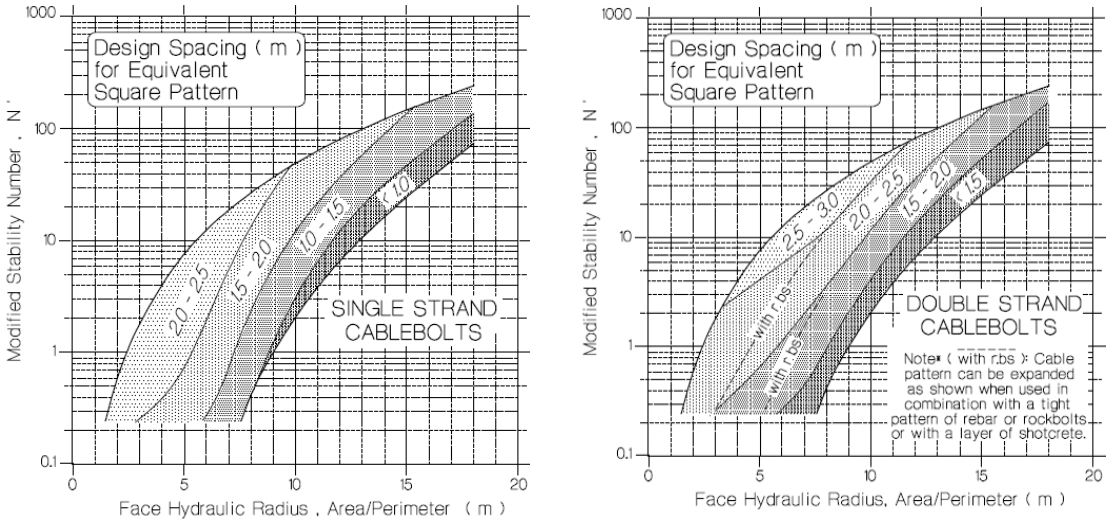


**Figures 16a and 16b. Cablebolt design stability graphs (Diederichs et al., 1999): (a) single strand bolts (b) single/double strand bolts**

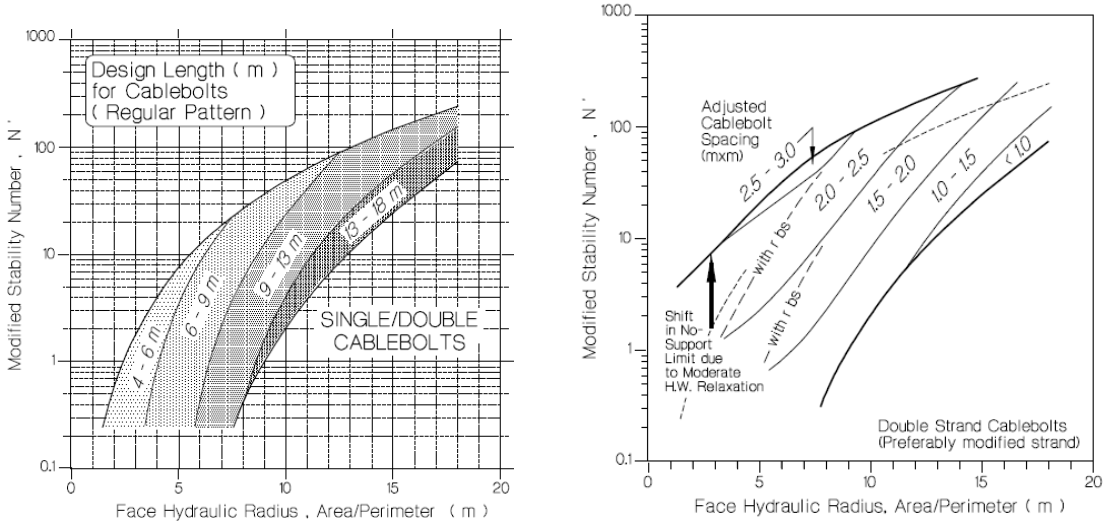


**Figures 16c and 16d. Cablebolt design stability graphs (Diederichs et al., 1999): (c) double strand and (d) adjusted bolt layout to account for partial relaxation.**

Fig. 17 is a likelihood statistic-based stability graph (Suorineni, 1998; Suorineni et al., 2001). In this figure a stope surface falling on a line with likelihood ratio (Λ) of 1 has equal chances of being stable and unstable. Each contour gives the likelihood of a stope surface to be stable, compared to it failing. Thus, a mine could select its stope sizes depending on the level of risk (dilution) it is willing to accept.

The likelihood ratio concept was applied to actual case histories in a Canadian hard rock underground mine where depths of stope wall failures were determined from cavity survey data. The likelihood ratios were back computed from Equation (9) and plotted against depths

of observed failure (Fig. 18). This figure shows that the higher the likelihood ratio, the smaller the depth of failure.

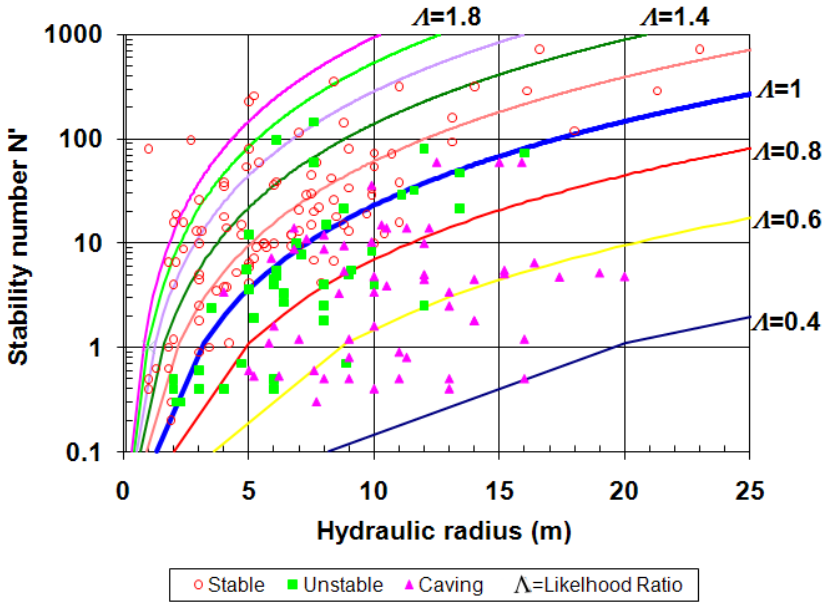


**Figure 17. Likelihood contours stability graph (Suorineni, 1998; Suorineni et al., 2001).**

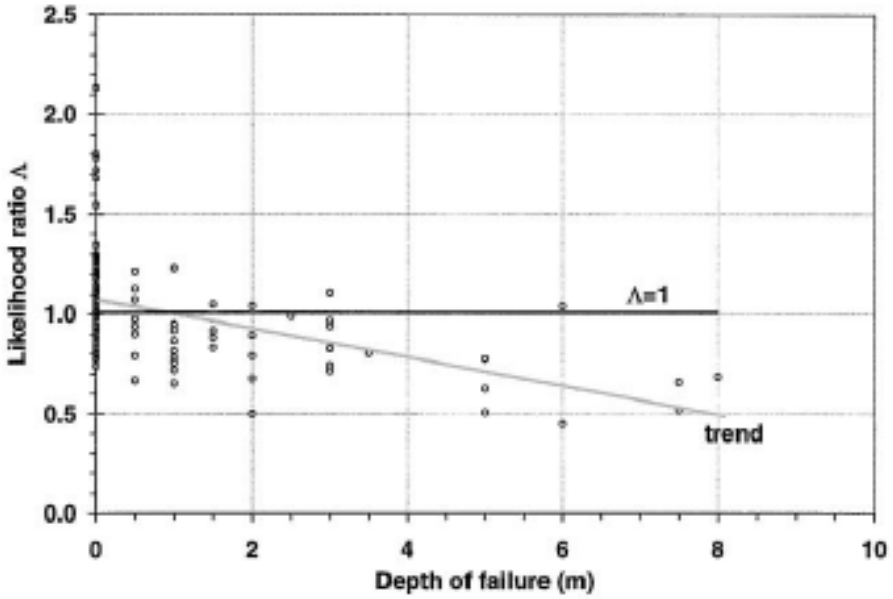


**Figure 18. Likelihood ratio versus depth of failure for depth of failure prediction (Suorineni, 1998).**

## 7. The stability graph and narrow vein mining

A major flaw in all the stability graph versions is that the stope surface stability states are not independent of orebody width. A stope hangingwall surface considered stable for an overbreak of 0.5 m in a massive orebody (say 10 m wide) is caving in a 1-m wide orebody. Thus the stability states defined in the stability graphs should account for orebody widths.

This flaw is assumed to exist because the stability graph was developed for mining massive orebodies, for which it is adequate.

Today, the stability graph application is extended to narrow vein mining without consideration for difference in definitions in the stope stability states for massive and narrow orebodies as demonstrated above. Unfortunately, the databases used for the development of the stability graphs exclude orebody geometries. Further work is required to correct this flaw.

Suorineni et al. (2001) used the stability graph to assess the performance of open stopes at the AngloGold-Ashanti Obuasi Mine. The Obuasi mine rocks are weaker than the rocks on which the original stability graph database was developed. It was established that the original stability graph transition zones do not apply to narrow vein stopes. Stewart et al. (2007) made similar observations in narrow vein mines in Australia and attribute this problem to backfill abutments and in-place natural pillars in narrow vein mines. However, the issues of backfill and in-place pillars are not unique to narrow vein mining alone but equally affect open stope mining in massive orebodies with backfill, and where secondary and tertiary pillar sequences are used.

Caceres (2005) investigated the effect of backfill on open stope stability design using the stability graph method. He concluded that a combination of the radius factors *RF* of the exposed and backfill parts of the stope surface should be used to account for the stability of the stope surface. This study only examined the stabilizing effect of the backfill on the rock walls of the stope, and did not address the fact that when some of the stope surfaces are made of backfill their instability has the potential to cause dilution in the stope to be mined. There is at present no procedure for assessing backfill wall stability in the stability graphs.

Backfill (e.g. cemented backfill) may be considered as a weak rock. $Q'$ in $N'$ (or $N$) does not apply to weak rocks. Løset (1999) notes that the Q-system is primarily suited for hard jointed rocks, with little case histories from weak rock (Q<1), especially squeezing and swelling rocks. The definition of weak rock is not unique, and is beyond the scope of this paper. With mines going deeper, and the use of backfill becoming essential and more common, there is need to establish procedures for incorporating backfill wall stability into the stability graph.

It is reiterated that the stability graph was developed for bulk mining of massive orebodies at depths below 1,000 m from surface. Mining of narrow vein orebodies results in tabular excavations with exposed long strike lengths of hangingwalls and footwalls or tall stopes in order to meet production targets. Long and tall stopes have the potential of resulting in deep relaxation zones in stope walls (at least in the Canadian Shield where $\sigma_1$ is horizontal). The consequence is large wall convergence that takes a significant portion of the stope width that can lead to ore hang-up in stopes, and excessive dilution. Thus, factors relevant for the stability of massive orebody open stopes do not have the same weight in controlling narrow vein open stopes stability. Narrow vein mining is also more prone to blast induced damage because of high confinements.

The databases of massive (wide) and narrow vein orebodies cannot be combined unless the overbreak or dilution is normalized to orebody widths. Hence, the stability graph with the combined Australian and Canadian databases, just as the ELOS stability graph (Section 6.2), should be used with caution, bearing in mind the wide variation in stope surface shape factors, which are a reflection of the range of the orebody widths.

## 8. Conclusions and recommendations

The stability graph was introduced nearly three decades ago for the design of open stopes in wide orebodies at depths below 1000 m. It is now a widely accepted method for open stope design in many mines around the world. The original database on which the method was developed was very limited (26 cases from 3 mines). Consequently, there was little confidence in the method until the database was expanded to about 175 cases from 34 mines. Expansion of the database resulted in modifications of the original stability number factors. Because the reliability of an empirical method of design depends on the size and quality of its database, conventional wisdom dictates that the modified stability number factors should be more reliable.

Review of the literature shows that there are two schools of thought when it comes to choice of factors for calculating the stability number (N). One group favours the original stability graph factors by Mathews et al. (1981), while another is in favour of the modified factors by Potvin (1988). The tendency for authors to arbitrarily choose between the original and modified stability number factors result in incomparable data that cannot be combined.

Some new adjustment factors such as fault factor, stand-up time and tension have also been introduced to improve the reliability of the stability graph in predicting stope performance. In situations where these new factors have been used, it should be clearly stated and the conditions given. This is important for the calibration and fine tuning of these new factors.

Differences exist in the definitions of stope stability state transition zones, depending on which version of stability graph is used. These differences result in different interpretations of the stability state of given stopes depending on the stability graph version used, and hence can be confusing.

Use of the stability graph is further complicated by the emergence of many other different types of stability graphs. There is the conventional stability graph, ELOS stability graph, cablebolt design stability graph, and risk-based stability graphs. Users of the stability graph should know the purpose for which they want to use it, and choose the stability graph that best suits their objective. This can be achieved by knowing and understanding the databases from which these stability graphs are developed. Empirical design methods are useful only when they are applied to conditions similar to those from which they were developed.

The stability graph boundaries are best defined by statistical procedures. Statistically defined boundaries eliminate unknown human error, and bias, with known predictive risks. The likelihood approach in discriminant analysis has the ability to define the stability graph transition zones, determine misclassification errors and apply risk / cost analysis to stope design in the stability graph. It is shown by Trueman and his co-workers that logistic regression is equally capable in achieving the same results as the likelihood statistic.

It is argued that individual mines develop their own stability graphs calibrated to suit their mining environments. While this is a welcome idea in the interpretation of empirical data there is much to gain in unifying the stability graph zones for general applications. As an empirical design procedure, the reliability of the stability graph is largely dependent on the size and quality of the calibration database. Such a database should be consistent with the stability number and shape factors determined in a consistent manner. Such a unified stability graph should define the stability graph zones taking into account the orebody widths from the data sources.

The stress factor *A* and gravity factor *C* do not account for increased stability of stope surfaces in moderate stress conditions due to potential for wedge clamping, nor do they account for rockbridges. In blocky rock masses with either tensile strength or in which

confinement exist above the critical value (0.2 to 0.5 MPa), the gravity factor cannot be independent of the stress factor *A*. Further work is required to establish this association. The lack of association between factors *A* and *C* is the likely source of the difficulty in establishing an acceptable *C* factor, and the misclassification of some stope surfaces.
In its current form, the gravity factor does not work for footwalls, and even though it is implied it applies to hangingwalls with dips ranging from 0˚ to 90˚, the database contains hangingwalls with dips in the range of 60˚ to 80˚ approximately. Hence, *C* should be applied with caution when dealing with hangingwalls with dips outside this range.

Additional factors have been developed, and incorporated into the determination of the stability number. In the past, the lack of a fault factor in the determination of the stability number was one of the most common criticisms against the method. Experience with the use of the stability graph showed that stope surfaces near faults often classify as stable but cave in service. The introduction of the fault factor minimizes the risk of over design of stopes near faults.

The argument that blast-induced damage is accounted for in the stability graph is not valid since no induced fractures are allowed to be included in the determination of rock mass quality. Hence, the effect of blasting should be accounted for in *N*. This could be achieved by including induced fractures in determining *Q'*. At present, blasting damage is accounted for in ELOS by assuming a constant blast damage value of 0.5 m. The severity of blast damage depends on blasting practice, types of explosive used, among others. Hence the assumption of adding a constant blast damage value to ELOS to account for blast damage is an over simplification. More work is required to validate these approaches.

There is overwhelming evidence that excavation stability is time-dependent. The time-dependence of open stopes stability is recognized by several authors. Accounting for time-effects in the stability graph is difficult but essential, and more effort is required in this direction. *ESR* should be considered in accounting for time in the stability graph.

The original stability graph was developed for bulk mining of massive orebodies, but has since been used for design of open stopes in narrower orebodies. The definitions of stability states in massive orebodies are not the same in narrow vein orebodies. A hangingwall described as stable in a massive orebody (10 m wide) for an overbreak / slough of 1 m, is

caved in a 1.5-m wide orebody. Hence, current versions of the stability graphs must be used with caution when applied to narrow vein orebodies, as they do not differentiate between wide and narrow vein orebodies.

Where backfill forms one of the surfaces of a stope the stability number *N* in its current form cannot be used to assess the stability of the stope surface, since *Q* does not apply to weak strength rock masses. Further research is needed to rectify this situation. The orientation (vertical or horizontal) of a rectangular hangingwall stope surface has an influence on dilution potential. The shape factor (HR) in the stability graph does not account for stope surface orientation effects. Consideration should be given to the inclusion of stope surface aspect ratio in the stability graph, particularly, when applied to the design of stopes in narrow vein orebodies.

**Acknowledgements**

The author wishes to thank Dr. J.G. Henning for proof reading the manuscript, his useful suggestions, and continuous support. Many thanks also go to Dr. C. Mawdesley, for giving the author a copy of her Ph.D. thesis during the literature review for this paper. I also wish to thank the anonymous reviewers for their valuable suggestions.

**References**

Barton, N., Lien, R. and Lunde, J. (1974), "Engineering classification of rock masses for the design of tunnel support", *Rock Mechanics*, Vol. 6 (1974), pp. 188-236.

Bawden, W.F., Nantel, J. and D. Sprott, D. (1989), "Practical rock engineering in the optimization of stope dimensions – Application and cost effectiveness", *CIM Bulletin*, Vol. 82, pp. 63-70.

Bewick, R. and Kaiser, P.K. (2009), "Numerical assessment of factor B in Mathews' method for open stope design", *Proc. 3rd CAN-US Rock Mechanics Symposium*, Toronto, 9-15 May, 2009, CD-ROM.

Bewick, R.P. (2008), *Effects of anisotropic rock mass characteristics on excavation stability*, M.A.Sc. thesis, School Engineering, Laurentian University, 187 p.

Bieniawski, Z.T. (1973), "Engineering Classification of Jointed Rock Masses", *Trans S. Afr. Inst. Civ. Engrs*, Vol. 15, pp. 335-344.

Bieniawski, Z.T. (1988), "The rock mass rating (RMR) system (Geomechanics Classification) in engineering practice", In *Rock Mass Classification Systems for Engineering Purposes*, Kirkaldie, L. (ed), ASTM, Philadelphia, pp. 13-34.

Brewis, T. (1995a), "Narrow vein mining 1 – Steep veins", *Mining Magazine*, pp.116-129.

Brewis, T. (1995b), "Narrow vein mining: 2 - flat-lying veins", *Mining Magazine*, pp. 129-133.

Caceres, C.A.B. (2005), *Effect of delayed backfill on open stope mining methods*, M.A.Sc. thesis, University of British Columbia, 152 p.

Canada Centre for Mineral and Energy Technology (CANMET), (1999), *Narrow-vein mining project*, http://mmsd1.mms.nrcan.gc.ca/canmet/description-e.asp.

Clark, L.M. (1998), *Minimizing dilution in open stope mining with focus on stope design and narrow vein longhole blasting*, M.A.Sc. thesis, University of British Columbia, 357 p.

Clark, L.M. and R.C. Pakalnis, R.C. (1997), "An empirical approach for estimating unplanned dilution from open stope hangingwalls and footwalls", *Proc. 99th Annual General Meeting, CIM*, Vancouver, B.C., Canada, 1997, CD-ROM.

Diederichs, M.S. and Kaiser, P.K. (1999), "Tensile strength and abutment relaxation as failure control mechanisms in underground excavations", *Int. J. Rock Mech. and Min. Sci.*, Vol. 36, pp. 69-96.

Diederichs, M.S. and Kaiser, P.K., (1996), "*Rock instability and risk analyses in open stope mine design", Can. Geotech. J.*, Vol. 33, pp. 431–439.

Diederichs, M.S., Hutchinson, D.J. and Kaiser, P.K. (1999), "Cablebolt layouts using the modified stability graph", *CIM Bulletin*, Vol. 92, pp. 81-86.

Dirige, A.Ph.E. (1996), "A proposed procedure for preliminary mining method selection for narrow vein", *In Proc. Mine planning and Equipment Selection*, Brazil, pp. 7-11.

Dominy, S.C. and Camm, G.S. (1996), "The nature and exploitation of narrow tin veins: A case study from South Crofty mine, Cornwall, U.K", *British Mining*, Vol. 57, pp. 150-170.

Dominy, S.C., Annels, A., Camm, G.S., Wheeler, P. and Barr, S.P. (1999), "Geology in the resource and reserve estimation of narrow vein deposits", *Explor. Geol*, Vol. 6., pp. 317-333.

Dunne, K. and R. Pakalnis, R. (1996), "Dilution aspects of a sublevel retreat stope at Detour Lake Mine", *Proc. 2nd North American Rock Mechanics Symposium*, Montreal, 19-21 June, 1996, pp. 305-313.

Evans, W.H. (1941), "The strength of undermined strata", *Trans. Instn. Min. Metall*., Vol. 50, pp. 475 – 500.

Finkel, M., Olsson, M., Thorshag, H., Wernström, J. and Johannson, G. (2001), "Narrow ore mining in Zinkgruvan, Sweden", *Chapt. 23, Underground Mining Methods – Engineering Fundamentals and International Case Studi*es, Hustrulid, W.A. and Bullock, R.L. (eds), SME (2001, pp. 221-227.

Finkel, M., Olsson, M., Thorshag, H., Wernström, J. and Johannson, G. (1987), *SveBeFo Report on Narrow ore Mining in Zinkgruven, Sweden*.

Germain, P. and Hadjigeorgiou, J. (1998), "Influence of stope geometry on mining performance", *Proc. 100th Annual General Meeting, CIM,* Vancouver, B.C., Canada, 1998, CD-ROM.

Germain, P., Hadjigeorgiou, J. and Lesard, J.F. (1996), "On the relationship between stability prediction and observed stope overbreak", *Proc. 2nd North America Rock Mechanics Symp.*, Aubertin M, Hassani F, Mitri H (eds), Quebec, 1-7 July, 1996, pp. 277–283.

Goodman, R.E. (1989), *Introduction to Rock Mechanics*, Second Edition, John Wiley and Sons, New York, 289 p.

Hadjigeorgiou, J., Leclaire, J. and Potvin, Y. (1995), "An update of the stability graph method of open stope design", *Proc. 97th Annual General Meeting, CIM Rock Mechanics and Strata Control session,* Halifax, Nova Scotia, 14-18 May, 1995, CD-ROM.

Henning, J.G. (2010), "Personal communication".

Henning, J.G. and Mitri, H.S. (2006), "Numerical modelling of ore dilution in blasthole stoping", *Int. J. Rock Mech. Min.,* Vol. 44, pp. 692–703.

Heslop, T.G. and Dight, P.M. (1993), "A review of geotechnical considerations in narrow vein mining in a high stress environment", *Proc. Narrow Vein Mining Seminar,* Bendigo, Victoria, Australia, Strakos V., Kebo, V., Farana, R. and Smutny, L. (eds), pp. 35-43.

Hoek, E. and Brown, E.T. (1980), *Underground Excavation in Rock,* Institution of Mining and Metallurgy, London, 527 p.

Hoek, E., Carranza Torres, C.T. and Corkum, B. (2002), "Hoek-Brown failure criterion: 2002 edition", *Proc. 5thNorth American Rock Mechanics Society Meeting*, Hammah, R., Bawden, W., Curran, J. And Telesnicki, M. (eds), Toronto, Canada, 7-10 July, 2002, Vol. 1, pp. 267-273.

Hutchinson, J.D. and Diederichs, M.S. (1996), *Cablebolting in Underground Mines*, Bitech Publishers, Ltd., Richmond, 406 p.

ISRM, (1981), *Rock Characterization, Testing & Monitoring: ISRM Suggested Methods*, Brown, E.T (ed), Pergamon, London, 211 p.

Kaiser, P.K., Falmagne, V., Suorineni, F.T., Diederichs, M.S. and Tannant, D.D. (1997), "Incorporation of rock mass relaxation and degradation into empirical stope design", *Proc. 99th Annual General Meeting*, Vancouver, B.C., Canada, April,1997, CD-ROM.

Laubscher, D.H. (1990), "Geomechanics classification of jointed rock masses – mining applications", *Trans. Instn Min. Metall.*, Vol. 86, pp. A1-8.

Lizotte, Y.C. (1993), *Narrow vein blasthole stoping: Current drilling and blasting Technology*, Project Report Submitted to The Canada Northwest Territories Mineral Development Agreement, 28 p.

Løset, F. (1997), *Use of the Q-method for securing small weakness zones and temporary support*, NGI Internal Report No. 548140-1, 40 p.

Løset, F. (1999), *Use of the Q-system in weak rock masses*, NGI report No. 592048-1, 44 p.

Martin, C.D. (1997), "*The effect of cohesion loss and stress path on brittle rock strength", Can. Geotech. J.* Vol. 34, pp. 698-725.

Mathews, K.E., Hoek, E., Wyllie, D.C. and Stewart, S.B.V. (1981), *Prediction of stable excavation spans at depths below 1000m in hard rock mines*, CANMET Report DSS Serial No. OSQ80-00081, 127 p.

Mawdesley, C. (2002), *Predicting rock mass cavability in block caving mines*, Ph.D. thesis, The University of Queensland, Brisbane, Australia, 256 p.

Mawdesley, C., Trueman, R. and Whiten, W. (2001), "Extending the Mathews stability graph for open-stope design", *Trans. Instn Min and Metall. (Section A: Mining Industry),* Vol. 110, pp. A27-39.

Mawdesley, C.A. (2004), "Using logistic regression to investigate and improve an empirical design method", *Int. J. Rock Mech. Min. Sci.*, Vol. 41, *CD-ROM*, 18-21 May, 2004, 6 p.

Miller, F., Potvin, Y. and Jacob, D. (1992), "Laser measurement of open stope dilution", *CIM Bulletin*, Vol. 85, pp. 96-102.

Milne, D. and Pakalnis, R.C. (1997), "Theory behind empirical design techniques", *12e Colloque en Contrôle de Terrain de l'Association Miniére du Quebéc*, Val d'Or, Quebéc, 1997, 20 p.

Milne, D., Pakalnis, R., Grant, D. and Sharma, J. (2004), "Interpreting Hanging Wall deformation in mines", *Intl. J. Rock Mech. & Min. Sci.,* Vol. 41, pp. 1139-1151.

Milne, D., Pakalnis, R.C. and Felderer, M. (1996), "Surface geometry assessment for open stope design", *Proc. 2nd North America Rock Mech. Symp,* Montreal, 1996, Vol. 1, pp. 315 – 322.

Nicholas, D.E. (1981), "Method selection – A numerical approach", *In Design and Operation of caving and Sublevel stoping Mines,* Stewart, D. (ed), New York, SME-AIME, pp. 39-54.

Nickson, S.D. (1992), *Cable support guidelines for underground hard rock mine operations,* M.A.Sc. thesis, University of British Columbia, 223 p.

Pakalnis, R.C. (1986), *Empirical stope design at Ruttan Mine*, Ph.D. thesis, University of British Columbia, 276 p.

Potvin, Y. (1988), *Empirical open stope design in Canada*, Ph.D. thesis, University of British Columbia, 343 p.

Potvin, Y. And Hadjigeorgiou, J. (2001), "The stability graph method for open-stope design", In *Underground Mining Methods: Engineering Fundamentals and International Case Studies*, Hustrulid,W., and Bullock, R. (eds), SME, Colorado, pp. 513 – 520.

Potvin, Y. and Milne, D. (1992), "Empirical cable bolt support design", *Proc. Int. Symp. Rock Mech.*, Sudbury, Ontario, Canada, pp. 269 - 275.

Ran, R. (2002), "Hanging wall sloughing mechanism in open stope mining", *CIM Bulletin*, Vol. 95, pp. 74-77.

Scoble, M.J. and Moss, A. (1994), "Dilution in underground bulk mining: Implications for production management", *Mineral Resource Evaluation II, Methods and Case Histories, Geological Society Special Publication*, Vol. 79, pp. 95-108.

Sofianos, A.I. (1996), "Analysis and design of an underground hard rock voussoir beam roof", *Int. J. Rock Mech. Min. Sci. and Geomech. Abstr.*, Vol. 33, pp. 153-166.

Sprott, D.L., Toppi, M.A. and Yi, X.P. (1999), "The incorporation of stress induced damage factor into Mathew's stability graph", *Proc. 101stCIM-AGM, Calgary*, 2-5 May, 1999, CD-ROM.

Stewart, P. and Trueman, R., Lyman, G. (2007), "Development of benchmark stoping widths for longhole narrow-vein stoping", *Mining Technology: IMM Transactions section A*, Vol. 116, pp. 167-175.

Stewart, P.C. and Trueman, R. (2003), Applying the extended Mathews stability graph: Quantifying case history requirements and site–specific effects, *1st AGCM Conference*, Sydney, Australia, 10-13 November, 2003, pp. 55-61.

Stewart, S.B.V. and Forsyth, W.W. (1995), "The Mathews Method for Open Stope Design", *CIM Bulletin*, Vol. 88, pp. 45-53.

Suorineni, F.T. (1998), *Effects of faults and stress on open stope design*, Ph.D. thesis, University of Waterloo, 362 p.

Suorineni, F.T., Henning, J.G. and Kaiser, P.K. (2001), "Narrow-vein mining experiences at Ashanti: Case study", *Proc. Inter. National Symp. Mining techniques of Narrow-vein Deposits,* Val'Dor, 2001, CD-ROM.

Suorineni, F.T., Henning, J.G. and Kaiser, P.K. (2008), "Safe rapid drifting - Support selection", *Tunnelling and Underground Space Technology,* Vol. 23, pp. 682-699.

Suorineni, F.T., Tannant, D.D. and Kaiser, P.K. (1999a), "Determination of fault-related sloughage in open stopes", *Int. J. Rock Mech. & Min. Sci.,* Vol. 36, pp. 891-906.

Suorineni, F.T., Tannant, D.D. and Kaiser, P.K. (1999b), "Fault factor for the stability graph method of open-stope design", *Trans. Instn. Min. Metall. (Sect. A: Mining Industry),* Vol. 108, pp. A92-104.

Suorineni, F.T., Tannant, D.D. and Kaiser, P.K. (2001), "Likelihood statistic for interpretation of the stability graph for open stope design", *Technical Note Int. J. Rock Mech. and Min. Sci.,* Vol. 38, pp. 735-744.

Suorineni, F.T., Tannant, D.D., Kaiser, P.K. and Dusseault, M.B. (2001), "Incorporation of a Fault Factor into the Stability Graph Method: Kidd Mine case Studies", *Mineral Resources Engineering*, Vol. 10, pp. 3-37.

Tannant, D.D. and Diederichs, M.S. (1997), *Cablebolt optimization in #3 Mine"*, Report to Shawn Seldon, Kidd Mines Division, Timmins, Ontario, Canada, 73 p.

Trueman, R. and Mawdesley, C. (2003), "Predicting cave initiation and propagation", *CIM Bulletin,* Vol. 96, pp. 54-59.

Trueman, R., Mikula, P., Mawdesley, C. and Haries, N. (2000), "Experience in Australia with the application of the Mathews method of open stope design", *CIM Bulletin.,* Vol. 93, pp. 162-167.

Wang, J.C. (2004), *Influence of Stress, Undercutting, Blasting and Time on Open Stope Stability and Dilution*. Ph.D., University of Saskatchewan, Saskatoon, 303 p.